Impact of Randomness of Wind Direction and Turbine Failure on Reliability Performance of Offshore Wind Farm

Angshu Plavan Nath
Dept. of Energy Sc. & Engg.
Indian Institute of Technology Bombay
Mumbai, India
nathangshu6@gmail.com

Zakir Hussain Rather
Dept of Energy Sc. & Engg.
Indian Institute of Technology Bombay
Mumbai, India
zakir.rather@iitb.ac.in

***Abstract*—This study analyses reliability of large scale offshore wind farm (OWF) while considering stochastic nature of both wind speed and wind direction as well as random failure of wind turbines (WT) in an OWF. Monte Carlo simulation has been used to incorporate random failure of WT into the study. To capture the stochastic nature of wind, markov chain has been used to generate synthetic time series data of both wind speed and wind direction for each iteration of the monte carlo simulation. The proposed methodology has been developed in MATLAB® and used for reliability analysis of Horns Rev-I OWF located in Denmark.**

***Index Terms*—Wake Effect, Offshore Wind Farm, Monte Carlo Simulation, Reliability**

I. Introduction

With increasing penetration of renewable sources into the electricity grid, reliability and security of power is one of the primary concerns. Stochastic sources, such as wind, has inherent availability constraints which introduces several challenges in the grid. As of 2018, wind generation has risen to 591 GW, of which 23 GW (4% of total) is from offshore wind farms (OWF) [1]. Due to prevalent grid based layout of WTs in OWF, wake effect plays a significant role in the power generation of OWF [2]. Wake is more pronounced when the inter-spacing distance between WTs is less, with more turbulence and lower wind speeds. As wind direction changes the inter-spacing distance between WTs along the direction of wind, consideration of wind direction along with wind speeds gains importance . Further, all WTs are liable for random failure which also adds to disturbances in the generating capacity of OWF. At any given time state, a WT can be either ON (1) or OFF (0) state. Also, once a WT fails, its downstream WT are not affected by its wake for the duration of its downtime, which has also been incorporated in this study.

In the literature, wake effect has been used for study of different operational characteristics of wind farms. The impact of wake in determination of inertia of an OWF has been carried out in [3]. On the other hand, authors in [4] used wake effect for optimized placement of WT in an OWF. Authors in [5] utilizes wake to propose a novel methodology of dispatch of reactive power in a wind farm. A comparison of markov chain (MC) and ARMA models for generation of time series wind data have been proposed in [6]. A two tier methodology using MC has been used in [7] to generate wind data considering day to day weather transitions and intra-day wind power fluctuations. The authors in [8] have studied correlation between WT failure and the stochastic variability of wind speed on wind farm reliability, but without considering the impact of wind direction. In [9], an economic and reliability model has been proposed for optimal layout of turbines in an OWF.

Based on the literature reported above, the key objectives of this study have been highlighted as under,

- Generation of synthetic wind speed and wind direction data for modeling of stochastic nature of wind.
- Use wake effect for calculation of power generating capability for different orientation of OWF as per the wind direction.
- Incorporate random failure of WT for reliability analysis of OWF while simultaneously considering wind variability and wake effect.

II. Methodology

A. Synthetic Wind Data Generation

Markov Chain modeling has been used in this study to generate synthetic wind speed and direction time series data with the same statistical properties as the original wind data. MC is a stochastic process that can be modeled after experimentally determining the probability of transition of one state to another [10]. As per Markov modeling, a transition matrix, TS with dimensions $m \times m$, where m is the number of states for wind speed/wind direction is initially formed from the wind data . The elements of the transition matrix are defined in (1).

$$ts_{ij} = \frac{\lambda_{ij}}{\sum_{j=1}^{m} \lambda_{ij}} \tag{1}$$

where, ts_{ij} are elements of TS, λ_{ij} is the frequency of transition of wind from state i to state j, of matrix TS. In other words, the transition matrix is a probability matrix where each element is the probability of transition from one state to

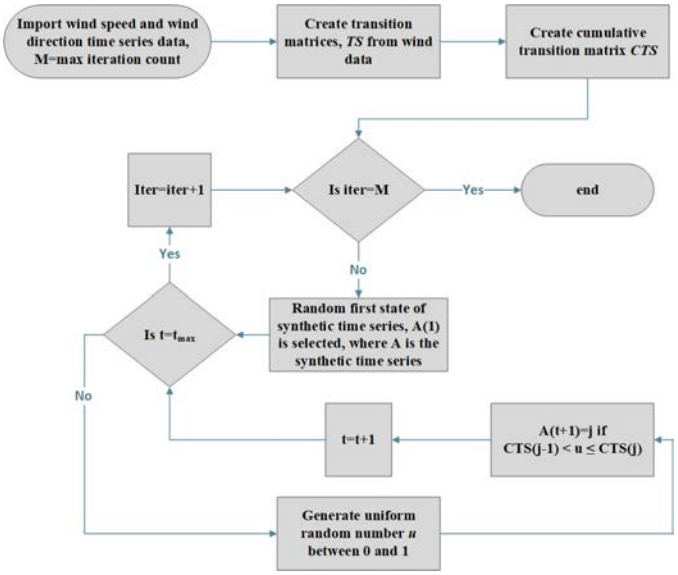

Fig. 1. Flow Chart showing the generation of synthetic time series using MC

another. As such, the summation of transition elements of each row should be equal to one as given in (2).

$$\sum_{j=1} ts_{ij} = 1 \tag{2}$$

For generation of the synthetic time series data, inverse transform method has been used. Cumulative probability transition matrices CTS is formed from TS. The initial state of the time series, say i is randomly selected, where $1 < i < m$. After the selection of the starting state, a uniform random number u, between 0 and 1 is selected. The next state in the synthetic time series is j if $CTS_i(j-1) < u \leq CTS_i(j)$, where CTS_i is the i^{th} row of the CTS matrix.. For the third state in the synthetic time series, u is again randomly generated, but now instead of searching i^{th} row, j^{th} row is searched. This process is repeated till the required number of data points for the time series data is generated. In this study, using MC two different sets of data have been generated for each iteration, one for wind speed and another for wind direction. For wind speed, a state is defined as a bin of width 1 m/s and for wind direction a state is defined as a bin with width 15^0. The entire process of generation of synthetic time series wind data using MC has been illustrated in Fig. 1.

B. Wake Effect

Wake effect in this study has been modeled using the Jensen's wake model. This wake model is well regarded in the literature as being one of the standard models to simulate wake effect inside an OWF as it produces comparable results to actual wake generated at distances greater than four times rotor diameter [11]. As per this model wake expands linearly with distance as given in (3) and shown in Fig.

$$r_w = R_{wt} + \gamma x \tag{3}$$

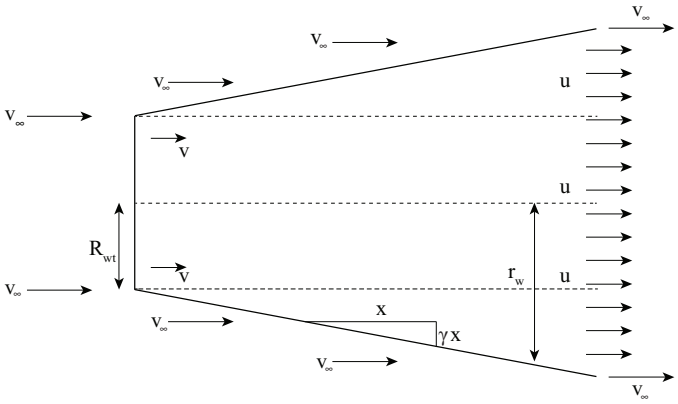

Fig. 2. Wake expansion by Jensen Method

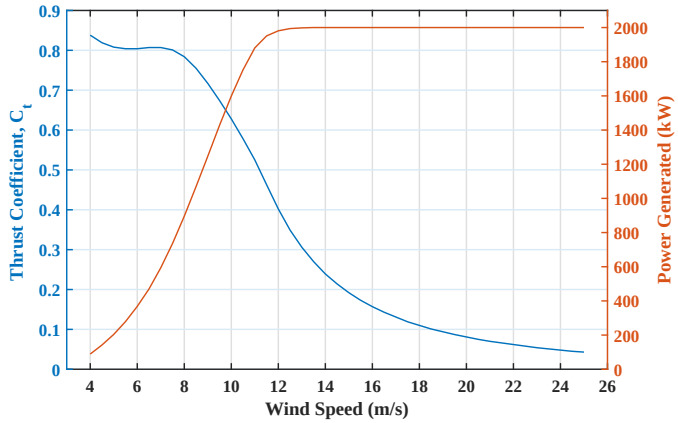

Fig. 3. Power generation curve and thrust coefficient curve of WT used in this study

where, r_w is the radius of wake at distance x, R_{wt} is the radius of WT and γ is the wake expansion coefficient which is considered as 0.08 for this study [12]. The velocity profile due to a single wake is determined by (4)

$$u = v_\infty - v_\infty \left(1 - \sqrt{1 - C_t}\right) \left(\frac{R_{wt}}{r_w}\right)^2 \tag{4}$$

where, u is wake velocity at distance x from WT, v_∞ is the free wind stream velocity, C_t is the thrust coefficient of the WT, the value of which is dependent on incident wind velocity and provided by turbine manufacturer and shown in Fig. 3. In an OWF, a WT is affected by multiple wakes from its upstream WTs. The incident wind speed due to presence of multiple wakes is given in (5).

$$v_j = \sqrt{v_\infty^2 - \sum_{i=1}^{M} \left(v_\infty^2 - v_{ij}^2\right) \left(\frac{S_j^i}{S_t}\right)} \tag{5}$$

where, v_j is incident wind speed on turbine j, M is the number of turbines, v_{ij} is the wind velocity on turbine j due to wake by turbine i and S_j^i is the overlapping area of wake by turbine i on rotor swept area of turbine j and S_t is the swept area of WT.

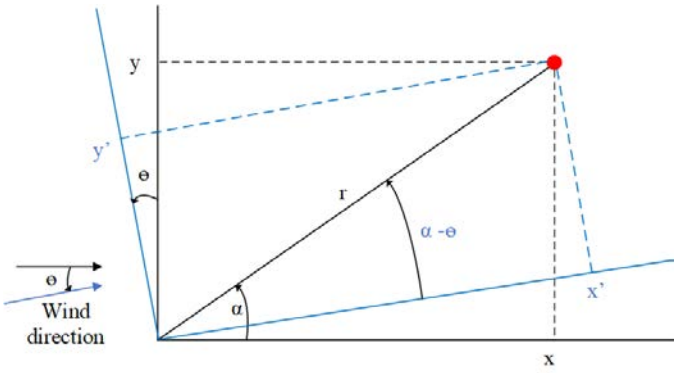

Fig. 4. Change in WT co-ordinates due to change in wind direction

C. Inclusion of Wind Direction

As mentioned in Section II-B, the impact of wake depends on the distance between WTs in an OWF, and on changing the direction of wind, the inter-spacing distance between WTs change. In effect, wind direction plays a significant role in determine the generation of an OWF. For incorporating wind direction in this study, the OWF is rotated by θ degrees everytime the wind direction changes, where θ is the wind direction at any time t. The co-ordinates of all WTs inside OWF is initially determined when wind direction is 0^0. If the initial co-ordinates of WT_i is considered as (x_i, y_i), it changes to (x_i', y_i') when wind direction is changed to θ (shown in Fig. 4) and can be calculated as shown in (6).

$$\begin{bmatrix} x_i' \\ y_i' \end{bmatrix} = \begin{bmatrix} cos\theta & sin\theta \\ -sin\theta & cos\theta \end{bmatrix} \times \begin{bmatrix} x_i \\ y_i \end{bmatrix} \tag{6}$$

D. Random Failure of Wind Turbines

WT are liable to random unscheduled failure. Sequential Monte Carlo (SMC) has been used in this paper to account for such failures, which has been explained in detail in [13]. In SMC, a $t \times s$ failure matrix, populated with either 1s or 0s (1s denoting operation state and 0s denoting non-operational states) is constructed for each iteration of the SMC simulation where, t is the number of WTs and s is the number of time states considered in each iteration. The probability of failure of a WT is based on historical data given in Table I [14]. Further, a WT requires a minimum downtime after failure for maintenance, before it is operational again. This duration has been calculated using (7).

$$Time_{down} = -MTTR \times ln(p) \tag{7}$$

where, $Time_{down}$ is the downtime following any failure, $MTTR$ is meantime to repair following any failure which is an empirical data calculated by averaging the repair times of all previous failures and p is a uniform random number between 0 and 1. Also, an non operational WT does not produce any wake, thereby minutely increasing the output of downstream WTs. The convergence criteria of the SMC simulation is defined such that the difference between mean loss of load percent (LOLP) of subsequent states is less than 10^{-5}.

TABLE I
WT FAILURE PROBABILITY

Wind Speed	Normal (<19 m/s)	Extreme (>19 m/s)
Failure rate (#/yr)	6	36
Repair rate (#/yr)	130	36

E. Reliability Estimation

Different reliability indices have been introduced in the literature for reliability estimation. In this context, the reliability indices used in this study are described below,

1) Expected Energy Not Supplied: Expected Energy Not Supplied (EENS) is the amount of energy not supplied by OWF on account of WT failure and can be mathematically defined by (8). It is generally expressed in MWh/yr.

$$EENS = \sum \left(P^{OWF}(t) - P(t)\right) \times T \tag{8}$$

where, $P^{OWF}(t)$ is the OWF generation in time state t without considering failure of WT, $P(t)$ is the actual OWF generation and T is the duration of each time state.

2) Loss of Load Percent: Loss of Load Percent (LOLP) is the percentage of energy not generated by OWF due to failure of one or more WTs and can be mathematically determined using (9).

$$LOLP = 1 - \frac{\sum P(t)}{\sum P^{OWF}(t)} \tag{9}$$

3) Expected Demand Not Supplied: Expected Demand Not Supplied (EDNS) is the average loss of power for each failure of WT event and can be mathematically defined as (10). It can be expressed in MW.

$$EDNS = \frac{\sum \left(P^{OWF}(t) - P(t)\right) \times T}{\sum_{i=1}^{z} F(i)} \tag{10}$$

where, $F(i)$ is the duration of state for which $P(t) < P^{OWF}(t)$ and z is the total number of such states.

The entire methodology have been summarized in Fig. 5.

III. System Description

The proposed methodology has been implemented in MATLAB/SIMULINK to estimate reliability of Horns Rev - I OWF located in Denmark. Horns Rev - I has 80 Vestas WT of 2 MW capacity each with a spacing of seven rotor diameters between each WT and a shear of 7.2^0 as shown in Fig. 6 [11]. The WTs have cut-in, rated and cut-out wind speeds of 4 m/s, 13 m/s and 25 m/s respectively with a rotor diameter of 80 m and hub height of 70 m.

The available wind speed data was sampled at every 10 min interval for 1 year while the wind direction was sampled with a sampling interval of 1 min.

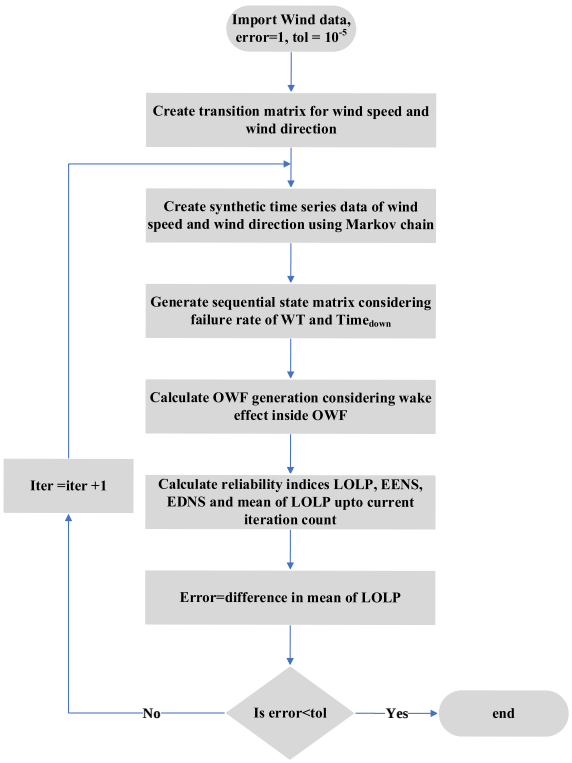

Fig. 5. Flow chart of the complete methodology

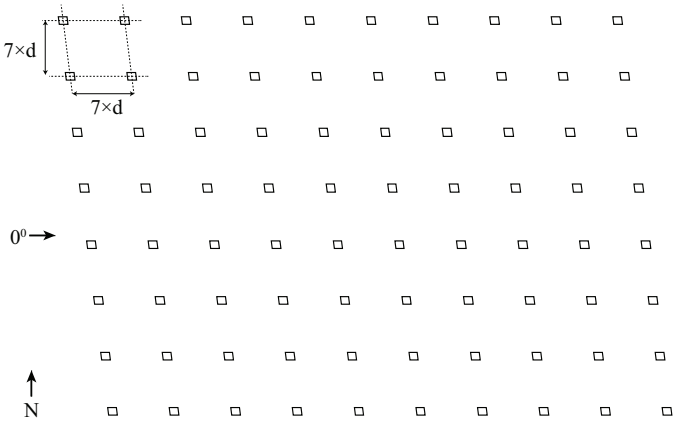

Fig. 6. Layout of Horn Rev-I OWF

IV. Results and Discussion

Synthetic wind speed time series data has been generated for each iteration of the SMC simulation for adequate modeling of the stochastic nature of wind, as described in Section II-A. The distribution of wind speed has been shown in Fig. 7 where, Fig. 7(a) shows the distribution of the actual wind data, while Fig. 7(b) and Fig. 7(c) distribution of two synthetic wind speed data (Series 1 and Series 2) generated for two different iterations shown here for illustrative purposes. It can be observed from Fig. 7, the generated wind speed data shows an expected Weibull distribution with shape (β) and scale (η) parameters given in Table II. Although β of Series 1 and Series 2 are comparable to the actual wind data, η of the Series 1 and Series 2 are slightly lower compared to actual data. This is because, the transition matrix generated from the wind speed data has been truncated for speeds greater than 21 m/s, as very few instances of such high speeds was recorded in the actual data which leads to creation of absorbing states. This resulted in a slightly skewed distribution curve of the generated synthetic time series.

Similarly, comparative wind rose diagram has been given in Fig. 8, where Fig. 8(a) is the wind rose of the actual data and Fig. 8(b) of the synthetic Series 1 data.

TABLE II
Weibull Parameters

Parameter	Actual	Series 1	Series 2
Shape (β)	2.461	2.188	2.246
Scale (η)	8.783	7.474	7.826

The OWF generation when considering same wind speed data, but for different specific directions shown in Fig. 9, have been given in Table III. It shows that among the different

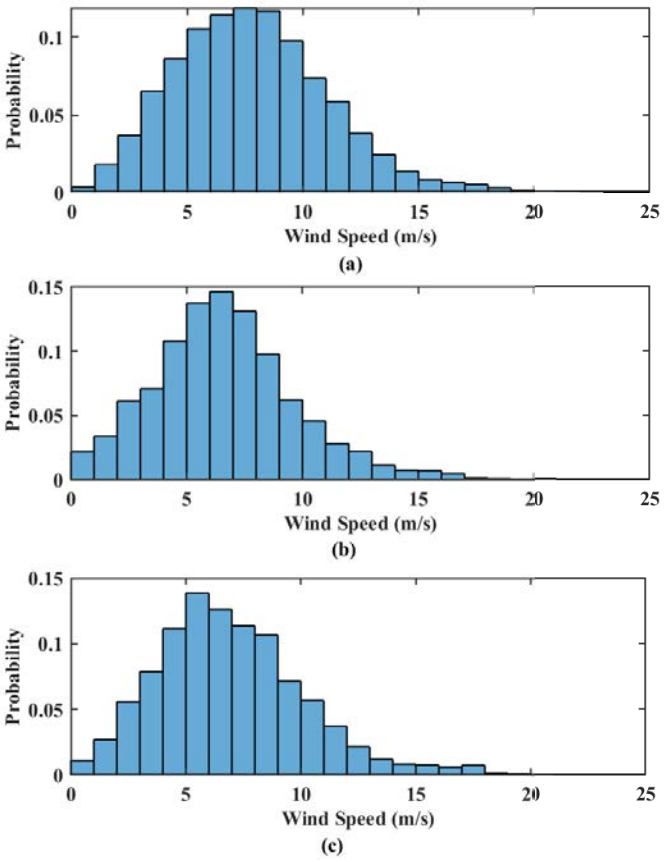

Fig. 7. Histogram showing the distribution of wind speed of (a) actual wind data, (b) synthetic time series of 1st iteration, (c) synthetic time series of 2nd iteration

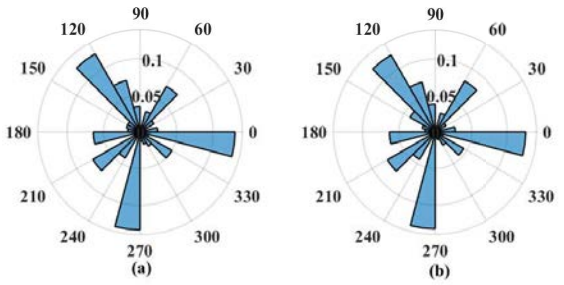

Fig. 8. Wind Rose of (a) Actual data (b) Series 1

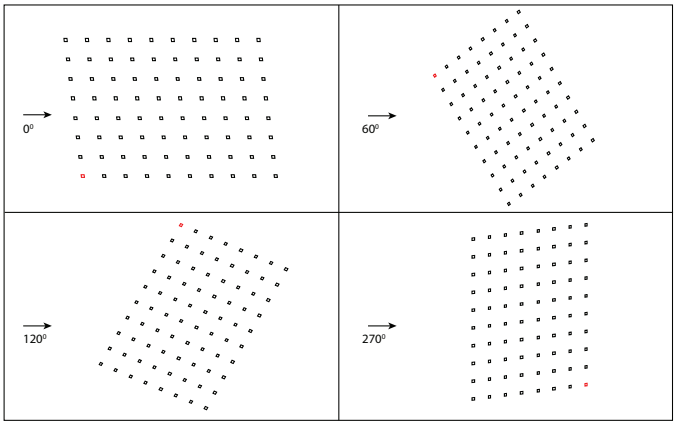

Fig. 9. Orientation of OWF for different wind directions

selected directions, 120^0 is the most favorable with the best performance, 60^0 and 270^0 have slightly lesser generation compared to 120^0, and with 0^0 being the least favorable direction with the worst performance. Power generation by OWF with and without consideration of wind direction is 384.4 ± 4.85 GWh and 312.7 ± 4.58 GWh respectively and has been shown in Fig. 10, where without direction means that the wind flow is from the initial 0^0 direction. The generation of OWF without consideration of wind direction is significantly lower than power generation with consideration of wind direction. This is because, the performance of OWF is relatively poor when wind direction is 0^0 as compared to other wind directions.

The OWF generation without consideration of random WT failure is 399.43 ± 5.00 GW as compared to 384.4 ± 4.85 GW with consideration of WT failure. Comparison of OWF generation with and without consideration of WT failure has been given in Fig. 11. OWF genertion under various considerations have been tabulated in Table IV.

TABLE III
OWF GENERATION FOR DIFFERENT DIRECTIONS WITHOUT CONSIDERING WT FAILURE

Direction	0^0	60^0	120^0	270^0
OWF Generation (GWh)	314.15	373.88	458.10	432.49

TABLE IV
OWF GENERATION UNDER DIFFERENT CONSIDERATIONS

Condition	Generation (GWh)
Without WT failure with Wind Direction	399.43 ± 5.0
With WT failure without Wind Direction	312.68 ± 4.58
With WT failure and with Wind Direction	384.4 ± 4.85

TABLE V
RELIABILITY INDICES

LOLP (%)	EENS (GWh/yr)	EDNS (MW)
3.76 ± 0.06	14.99 ± 0.28	2.43 ± 0.03

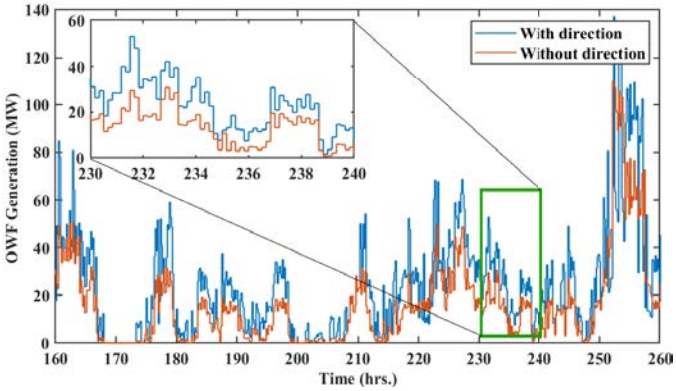

Fig. 10. Comparison of OWF generation with and without consideration of wind direction

From this study, it was found that the LOLP of the OWF was 3.76 ± 0.06 or in other words it was unable to generate 3.76% of its generation capability due to random WT failure. The EENS was calculated to be 14.99 ± 0.28 GWh/yr and the EDNS was 2.43 ± 0.03 MW i.e. throughout the 1 year period the OWF was unable to supply 14.99 GWh of energy due to WT failure and the average loss of power for each failure event was 2.43 MW. The reliability indices have been tabulated in Table V.

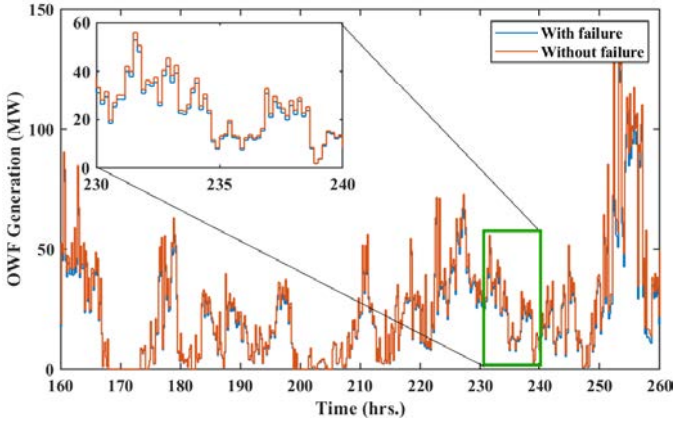

Fig. 11. Comparison of OWF generation with and without consideration of random WT failure

V. Conclusion

The estimation of OWF reliability with consideration of stochastic variability of wind speed, wind direction and random failure of WT have been proposed in this study. The applicability of MC for generation of stochastic wind data have been highlighted. A significant difference in OWF generation on consideration of wind direction is observed. This reinforces the importance of wind direction consideration for study of OWF. To characterize reliability of OWF, LOLP, EENS and EDNS have been used as indices.

Acknowledgment

This work has been supported by Shastri Indo-Canadian Institute under the project "Grid Stability of Large-Scale Renewable Energy Integrated Power System"

References

[1] GWEC, "Global wind report 2018," *GWEC, Brussels, Belgium, Technical Report*, 2019.

[2] S. Paul and Z. H. Rather, "A Pragmatic Approach for Selecting a Suitable Wind Turbine for a Wind Farm Considering Different Metrics," *IEEE Transactions on Sustainable Energy*, vol. 9, no. 4, pp. 1648–1658, 2018.

[3] H. Gu, "Wake effect in wind farm dynamic modelling," in *2017 Australasian Universities Power Engineering Conference (AUPEC)*, Nov 2017, pp. 1–5.

[4] P. Hou, W. Hu, M. Soltani, and Z. Chen, "Optimized placement of wind turbines in large-scale offshore wind farm using particle swarm optimization algorithm," *IEEE Transactions on Sustainable Energy*, vol. 6, no. 4, pp. 1272–1282, Oct 2015.

[5] J. Tian, D. Zhou, C. Su, Z. Chen, and F. Blaabjerg, "Reactive power dispatch method in wind farms to improve the lifetime of power converter considering wake effect," *IEEE Transactions on Sustainable Energy*, vol. 8, no. 2, pp. 477–487, April 2017.

[6] A. Bizrah and M. AlMuhaini, "Modeling wind speed using probability distribution function, markov and arma models," in *2015 IEEE Power Energy Society General Meeting*, July 2015, pp. 1–5.

[7] D. Li, W. Yan, W. Li, and Z. Ren, "A two-tier wind power time series model considering day-to-day weather transition and intraday wind power fluctuations," *IEEE Transactions on Power Systems*, vol. 31, no. 6, pp. 4330–4339, Nov 2016.

[8] N. Nguyen, S. Almasabi, and J. Mitra, "Impact of correlation between wind speed and turbine availability on wind farm reliability," *IEEE Transactions on Industry Applications*, vol. 55, no. 3, pp. 2392–2400, May 2019.

[9] Y. Wu, P. Su, Y. Su, T. Wu, and W. Tan, "Economics- and reliability-based design for an offshore wind farm," *IEEE Transactions on Industry Applications*, vol. 53, no. 6, pp. 5139–5149, Nov 2017.

[10] A. Shamshad, M. Bawadi, W. W. Hussin, T. Majid, and S. Sanusi, "First and second order markov chain models for synthetic generation of wind speed time series," *Energy*, vol. 30, no. 5, pp. 693–708, 2005.

[11] S. Kuenzel, L. P. Kunjumuhammed, B. C. Pal, and I. Erlich, "Impact of wakes on wind farm inertial response," *IEEE Transactions on Sustainable Energy*, vol. 5, no. 1, pp. 237–245, Jan 2014.

[12] F. González-Longatt, P. Wall, and V. Terzija, "Wake effect in wind farm performance: Steady-state and dynamic behavior," *Renewable Energy*, vol. 39, no. 1, pp. 329–338, 2012.

[13] A. Nath, S. Paul, Z. Rather, and S. Mahapatra, "Estimation of offshore wind farm reliability considering wake effect and wind turbine failure," in *2019 IEEE Innovative Smart Grid Technologies Asia*, In Press.

[14] H. Kim, C. Singh, and A. Sprintson, "Simulation and estimation of reliability in a wind farm considering the wake effect," *IEEE Transactions on Sustainable Energy*, vol. 3, no. 2, pp. 274–282, 2012.